AD-A099 039 WAYNE STATE UNIV DETROIT MI BIOENGINEERING CENTER F/G 6/19
MECHANISMS OF CERVICAL SPINE INJURY DURING IMPACT TO THE PROTEC--ETC(U)
MAR 81 V R HODGSON, L M THOMAS N00014-75-C-1015
UNCLASSIFIED TR-12 NL

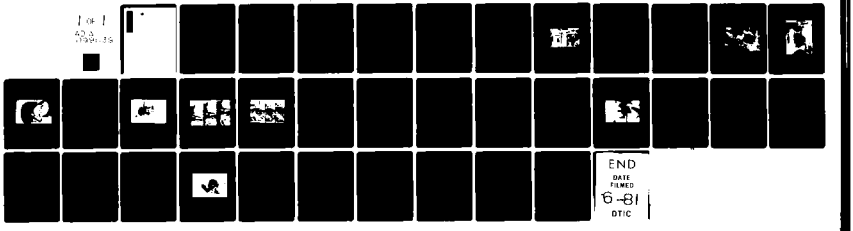

SECURITY CLASSIFICATION OF THIS PAGE (When Data Entered)

REPORT DOCUMENTATION PAGE

READ INSTRUCTIONS BEFORE COMPLETING FORM

1. REPORT NUMBER: N00014-75-C-1015	2. GOVT ACCESSION NO.: AD-A099 039
3. RECIPIENT'S CATALOG NUMBER:	
4. TITLE (and Subtitle): Mechanisms of Cervical Spine Injury During Impact to the Protected Head	5. TYPE OF REPORT & PERIOD COVERED: Technical Report 4/1/80 - 3/31/81
	6. PERFORMING ORG. REPORT NUMBER: Technical Report No. 12
7. AUTHOR(s): Voigt R. Hodgson and L. Murray Thomas (14) TR-12	8. CONTRACT OR GRANT NUMBER(s): N00014-75-C-1015
9. PERFORMING ORGANIZATION NAME AND ADDRESS: Wayne State University, Bioengineering Center 418 Health Science Building, Detroit, MI 48202	10. PROGRAM ELEMENT, PROJECT, TASK AREA & WORK UNIT NUMBERS:
11. CONTROLLING OFFICE NAME AND ADDRESS: Department of the Navy, Office of Naval Research Structural Mechanics Program (Code 474) Arlington, VA 22217 (12)	12. REPORT DATE: March 9, 1981 (11) 9 March 13. NUMBER OF PAGES: 36
14. MONITORING AGENCY NAME & ADDRESS (if different from Controlling Office): same as above	15. SECURITY CLASS. (of this report): Unclassified
(9) Technical Report, 1 Apr 80-31 Mar 81	15a. DECLASSIFICATION DOWNGRADING SCHEDULE:

16. DISTRIBUTION STATEMENT (of this Report)

Approved for public release; distribution unlimited.

17. DISTRIBUTION STATEMENT (of the abstract entered in Block 20, if different from Report)

Proceedings of the 24th Stapp Car Crash Conference; Society of Automotive Engineers, Transactions of the Society of Automotive Engineers, 1981.

18. SUPPLEMENTARY NOTES

This paper received the national 1980 Ralph H. Isbrandt Automotive Safety Engineering Award to be presented by the Society of Automotive Engineers in June, 1981.

19. KEY WORDS (Continue on reverse side if necessary and identify by block number)

biodynamic response, neck injury, head impact, protective helmets

20. ABSTRACT (Continue on reverse side if necessary and identify by block number)

Static and impact loading of the heads of embalmed cadavers wearing protective helmets have been conducted for the purpose of understanding the mechanics of fracture-dislocation injury to the cervical spine. Some of the cadavers were cut down on one side of the neck for high-speed photographic observation of the spine during impact. Others were instrumented with strain gages on the bodies and near the facets to assist in correlating spine movements and load configuration with strain distribution.

DD FORM 1 JAN 73 1473 EDITION OF 1 NOV 65 IS OBSOLETE

S/N 0102-LF-014-6601

SECURITY CLASSIFICATION OF THIS PAGE (When Data Entered)

Results indicate that static loading can be a useful predictor of failure site under dynamic conditions. Those conditions which were found to be most influential on injury site and level of strain were: 1) The extent to which the head was gripped by the impact surface to allow or restrict motion at the atlanto-occipital injunction; 2) Impact location; and, 3) Impact force alignment with the spine.

It was found that very little could be done with energy-absorbing material in the crown to reduce spine strain due to a crown impact. Also, the rear rim was not a 'guillotine' threat to fracture-dislocation from blows which cause hypertension, and the higher cut rear rim recommended to reduce or eliminate this alleged hazard caused higher strain by virtue of allowing greater extension of the neck.

S/N 0102-LF-014-6601

MECHANISMS OF CERVICAL SPINE INJURY DURING IMPACT TO THE PROTECTED HEAD

VOIGT R. HODGSON AND L. MURRAY THOMAS
WAYNE STATE UNIVERSITY
DETROIT, MI 48202

SUMMARY

Static and impact loading of the heads of embalmed cadavers wearing protective helmets have been conducted for the purpose of understanding the mechanics of fracture-dislocation injury to the cervical spine. Some of the cadavers were cut down on one side of the neck for high-speed photographic observation of the spine during impact. Others were instrumented with strain gages on the bodies and near the facets to assist in correlating spine movements and load configuration with strain distribution.

Results indicate that static loading can be a useful predictor of failure site under dynamic conditions. Those conditions which were found to be most influential on injury site and level of strain were: 1) The extent to which the head was gripped by the impact surface to allow or restrict motion at the atlanto-occipital junction; 2) Impact location; and, 3) Impact force alignment with the spine.

It was found that very little could be done with energy-absorbing material in the crown to reduce spine strain due to a crown impact. Also, the rear rim was not a 'guillotine' threat to fracture-dislocation from blows which cause hyperextension, and the higher cut rear rim recommended to reduce of eliminate this alleged hazard caused higher strain by virtue of allowing greater extension of the neck.

Most of the research on the mechanics of spinal injuries has been carried out on segments of the cervical spine. Notable in this respect has been the work of Roaf (1) who used the basic spinal unit consisting of two intact vertebrae joined by an intervertebral disc, two posterior articulations and a number of ligaments. Roaf found the disc, joints and ligaments to be very resistant to compression, distraction, flexion and extension, but very vulnerable to rotation and horizontal shearing forces. In general he found that rotation forces produce dislocations, and compression forces produce fractures.

Bauze and Ardran (2) devised an experiment in which entire cervical spines, with basi-occiput attached, were subject to compressive loads with the lower part of the spine flexed and fixed, and the upper extended and free to move forward. They loaded the specimen with a combination of vertical compression, flexion, and horizontal shear forces. Bilateral dislocation of the facets was produced without fracture with only 1.42 kN. They found that the maximum load coincided with the rupture of the posterior ligaments (interspinous and capsular) and stripping of the anterior longitudinal ligament prior to dislocation. In contrast to this, Roaf (1) found that the compressive strength of end plates of the vertebral bodies was around 6.23 kN and that the intact disc was even stronger, failing around 7.12 kN. When Roaf loaded the spinal unit in slight flexion and applied rotational force to the posterior ligaments, joint capsules and posterior longitudinal ligaments tore in that order resulting in a typical dislocation. However, he was unable to succeed in producing pure hyperflexion (when disruption of posterior ligaments occur) injury of a normal intact spinal unit. Before the posterior ligaments ruptured, the vertebral body always became crushed. These

experiments with segments of the cervical spine indicate that failure can be a complex process and the external load is not a good predictor of when failure will occur, what tissues will fail, and where the failure will occur.

The use of an entire human surrogate to study the response to axial compressive loads due to impacts on the crown were conducted by Mertz, et al. (3). A Hybrid III dummy was placed in an impact environment in which a football mechanical blocking and tackling device had allegedly produced paralyzing neck injuries. Axial compressive loading was primarily produced by impacts from the resilient foam-padded steel cylinder weighing 245 N to the crown of the dummy during the impact intensities assumed to have produced the injuries. This group published two reference curves, one for football players with a maximum value of 6.67 Kn, and another with a peak value of 4.45 kN for the adult population. They cautioned that since injury can occur under a variety of loading conditions, being below the curve does not necessarily insure that neck injury will not occur when the dummy is placed in a particular loading environment.

Culver, et al. (4), studied direct impact to the crown of fresh cadavers in which the subjects were placed in a supine position and the cervical spine was aligned along the impactor axis. These investigators found that the predominantly spinous process fractures produced in their setup indicated a compressive arching which followed the normal lordotic curvature of the cervical spine and appeared to depend on the initial rotation of the head and axial alignment of the spine. They found that if the head rotated rearward or the head was placed above the axis of the spine the arching was increased. No dislocations, no anterior compressive fractures of the bodies of the vertebrae, nor any basal skull fractures

were found. The data indicated that peak impact force of 5.7 kN is a level above which cervical spine fractures will begin to occur for an average cadaver under conditions of their experiment.

In addition to its inherent instability under the action of head impacts with a compressive compoment (crown impact), another primary reason for lack of understanding of cervical spine injury mechanisms due to crown impact has been the inability to visualize spine movements or quantify the effects of load variables. The present series was designed to enable visualization of parts of the spine by means of high-speed photography and measurement of vertebral strain during impact to the helmeted head of embalmed cadavers.

METHODS

Shown in Figure 1 is the device used by Mertz, et al. (3), to impact the Hybrid III dummy. In the present series, it was used to propel any of three surfaces consisting of the soft foam-filled padded steel cylinder of Mertz, a padded knee from a Sierra 1050 dummy, or a load cell, padded or unpadded. When fitted with either the similar weight (245 N) padded cylinder or knee, the impact mass could be propelled by three combinations of tension springs to velocities of 3 ms, 4.1 ms, or 5.2 ms, striking near the end of the allowable travel at which impact occurred. Using the load cell, the striking body weighed 445 N and moved at proportionately lower impact velocities.

The cadavers were strapped in a prone position to a 312 N aluminum pallet with provision for raising the chest and head to control the impact location. The pallet was placed on a roller-bearing conveyor such that the pallet was free to roll.

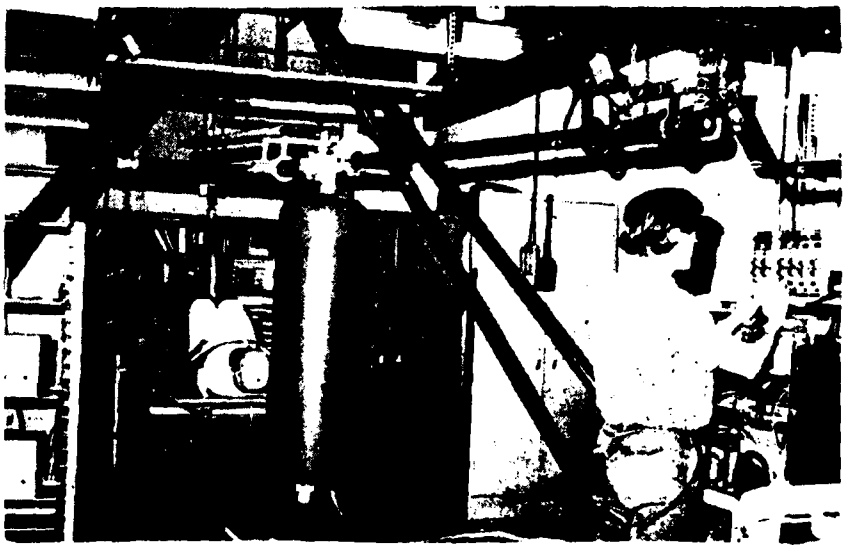

Fig. 1- Springloaded propulsion system used to deliver head impacts.

CADAVERS - Sixteen embalmed male cadavers were used in these tests. Most of the cadavers were prepared by sectioning the left side of the neck to expose parts of either the spinous processes or the bodies and facet joints. Preliminary experiments on several of these cadavers in which the entire sides of the vertebrae were exposed, including the bodies, facets, and spinous processes, produced predominantly lower cervical interspinous ligament failures which are atypical of cervical spine injuries seen clinically. Four of the cadavers were fitted with strain gages, beginning with three on the anterior surfaces of the bodies of C3, C5, and C7 on the initial cadaver, to as many as twelve on both the anterior surfaces of the bodies of all except C1 and near the left facet joints of all the cervical vertebrae. Although it was necessary to remove part of the longitudinal ligament at each anterior body gage site, this did not appear to weaken the spine. The cadavers were fitted with a protective helmet of the resilient linear type for the purpose of distributing the impacts, especially with the rigid load cell, to prevent skull fracture, and minimize variables resulting from skin damage.

OTHER INSTRUMENTATION - In a few cases the helmet was cut away and a triaxial accelometer was screwed to the cadaver skull for the purposes of measuring the resultant acceleration at the mounting location in the mid-sagittal plane. A LOCAM ^{R} and a HYCAM ^{R}, operating at 500 and 1000 fps, were used to record head and neck motion in selected cases. Velocity of the impact surfaces was measured by interception of two light beams within 25 mm of the impact site.

OTHER IMPACT SETUPS - Several tests used gravity propulsion of a cadaver strapped to a light pallet pivoted at the feet and allowed to

free fall into impact of the extended head to a Sierra 1050 knee surface which was free to swing away. This produced an I-S compoment of force with resulting hyperextension of the neck. Facemasks were used on the helmet to investigate whether or not an impact on the mask could, by virtue of a rear rim 'guillotinirg' mechanism, produce fracture and/or dislocation of the cervical spine: and/or whether a high cut rear rim was beneficial from the standpoint of reducing this hazard (Fig. 2).

STATIC TESTS - For optimum control of tests and to understand the dynamics of the spine, static load deflection tests were conducted as shown in Figure 3. The cadavers were seated in a frame under a hydraulic press operated at a slow loading rate of 10 mm/s. Scissor jacks were used to position and brace the body. A loading fixture was clamped to the head for the purpose of loading at discrete points through a clevis which could be fixed to prevent head rotation, simulating the gripping action of a distributed dynamic impact, or a free clevis that simulated the action of a concentrated impact allowing nodding at the atlanto-occipital joint.

RESULTS

DISTRIBUTED CROWN IMPACT - Shown in Figure 4 is an excerpt from film taken at 500 fps of a distributed impact to the crown of the helmet. The gripping action of the bag on the helmet minimized rotation of the head on the neck at the atlanto-occipital joint even though the impact was anterior to the cervical axis. This resulted in a configuration of the spine similar to the so-called "duckling" shape described by Bauze and Ardran (2), typically sustained when diving into a shallow, sandy bottom pool. The modes of failure in this situation occur in the lower cervical with the possibility of crushing the anterior bodies of C5 or

Fig. 2- Position at impact of facemask drop test onto swing-away dummy knee to observe effect of rear rim on spine strain.

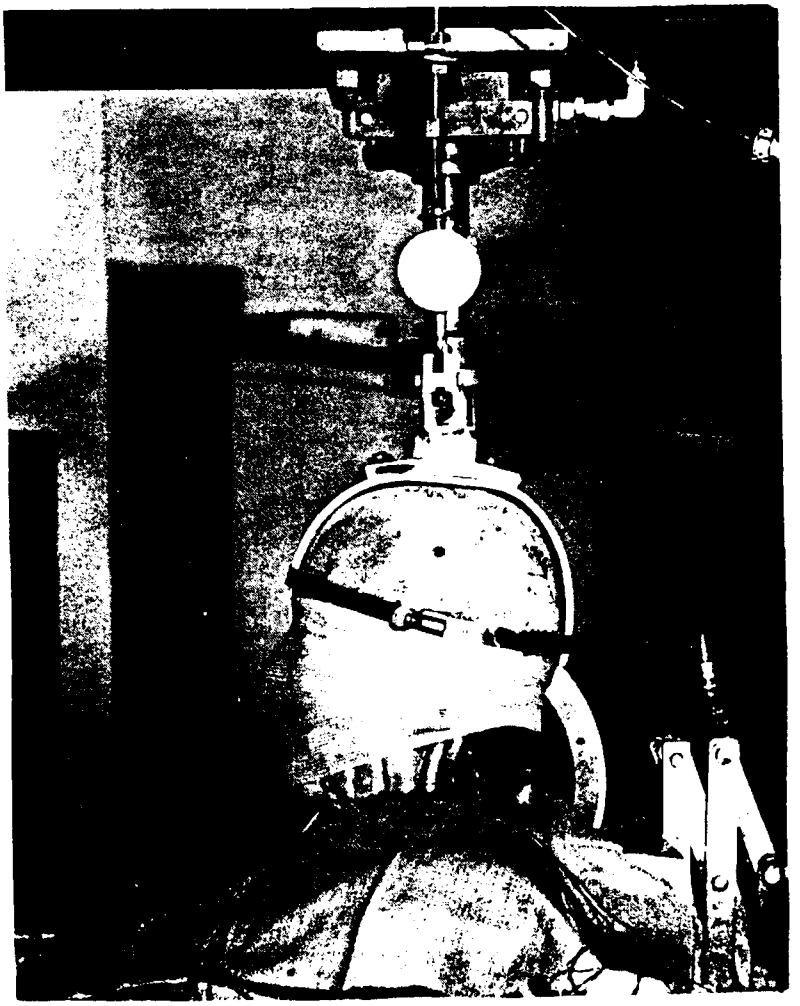

Fig. 3- Static test setup for appyling axial loads to head.

Fig. 4- Excerpt from film taken at 500 fps showing distributed impact and resultant "ducking" shape of the cervical spine.

C6, a forward dislocation of C5 over C6, or a possible tear of interspinous ligaments in the region of C5-C7.

CONCENTRATED IMPACT - Concentrated impact against such as a padded knee of the 1050 Sierra dummy shown in Figure 5 anterior to the cervical axis, allows head nodding at the atlanto-occipital joint with resultant high cervical flexion. As the flexion increases the shear component increases with the likelihood of a bilateral dislocation (2) in the event of symmetrical loading, or what is more likely, a unilateral dislocation due to compression-flexion-rotation loading. Such a unilateral dislocation is shown in the sequence of frames in Figure 6 (left to right) which displays the dislocation of the C2 facet on C3, ending in locked facets. This dislocation appeared to be caused by compression-flexion loading with resultant P-A shear stress and was followed rather than preceded by rotation as predicted by Roaf's setup (1).

STATIC TESTS - After conducting numerous tests with distributed and concentrated loading it became apparent that many modes of failure could occur depending on the orientation of the neck prior to impact. As pointed out by Bauze and Ardran (2), if a person lands on his head with the whole neck in extension, fractured spinous processes with ruptured anterior longitudinal or anterior avulsion fracture may be expected. This was evidently the experience of the Culver, et al., study in which spinous process and intervertebral ligament failure occured (4). Lateral flexion may produce rupture of the capsular ligaments around the middle of the neck on the convex side, as shown in the excerpt from high-speed film of C4-C5 separation in Figure 7 of the present series. This instability was afterward undetectable on x-ray as the joint returned to normal position. Experiences of these tests also indicated that if the

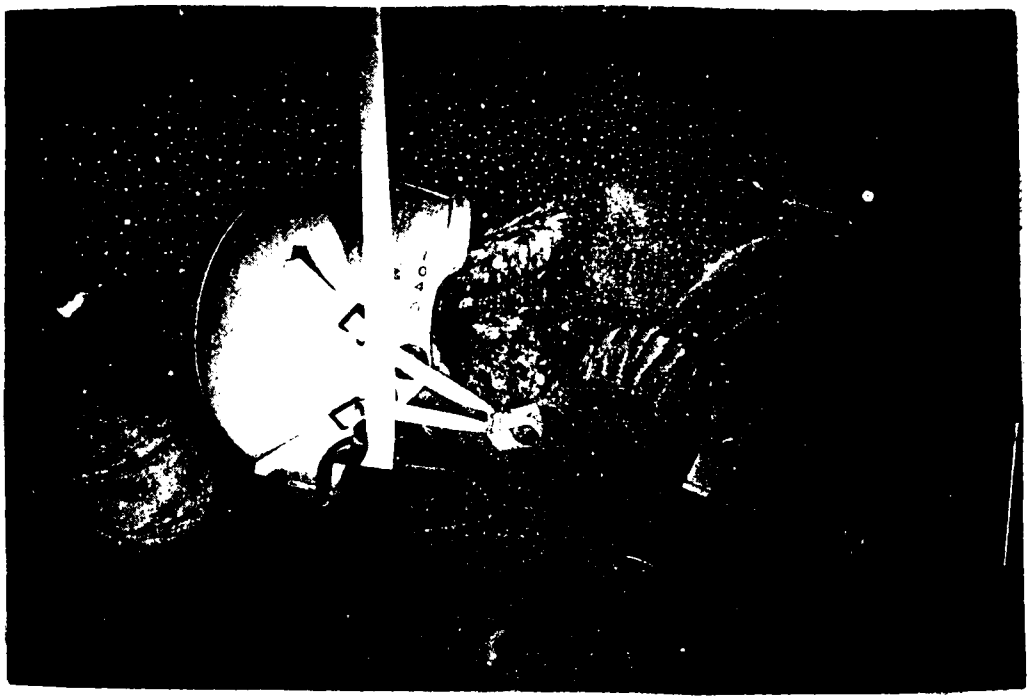

Fig. 5 - Concentrated load delivered by moving dummy knee to stationary cadaver anterior crown surface.

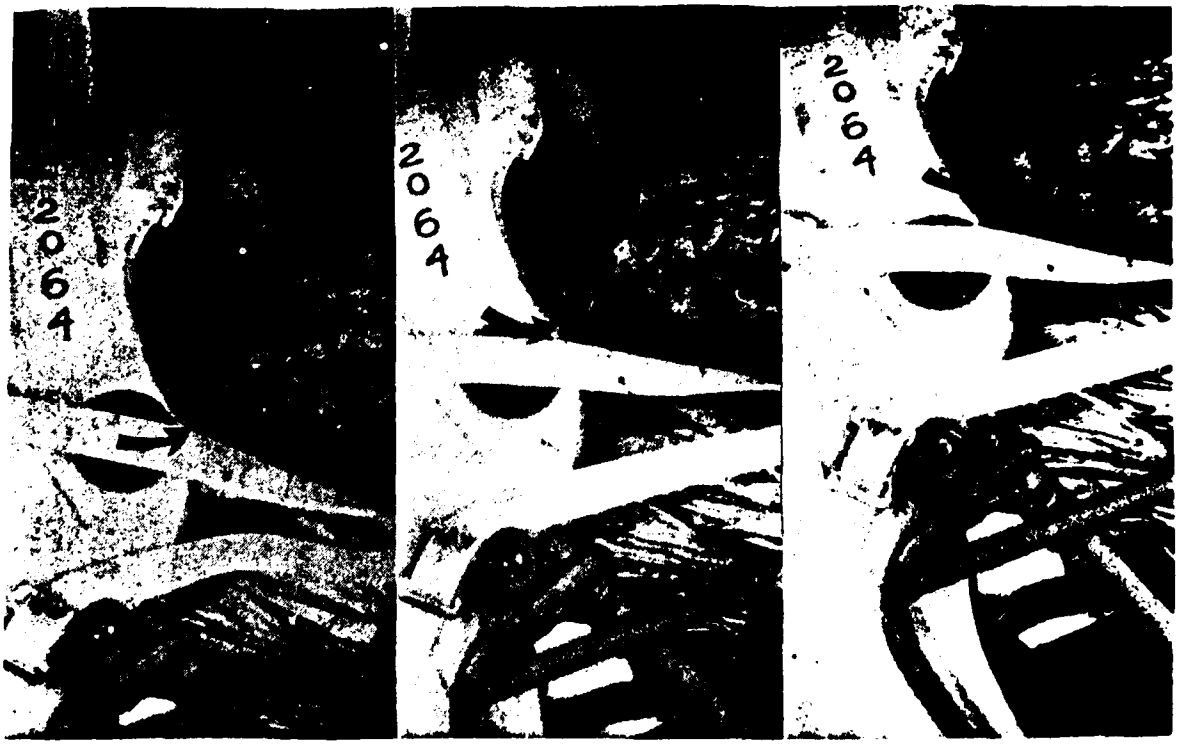

Fig. 6 - Excerpts from film taken at 500 fps showing the occurrence of a unilateral dislocation of C2 and C3 from a concentrated load anterior to the cervical axis.

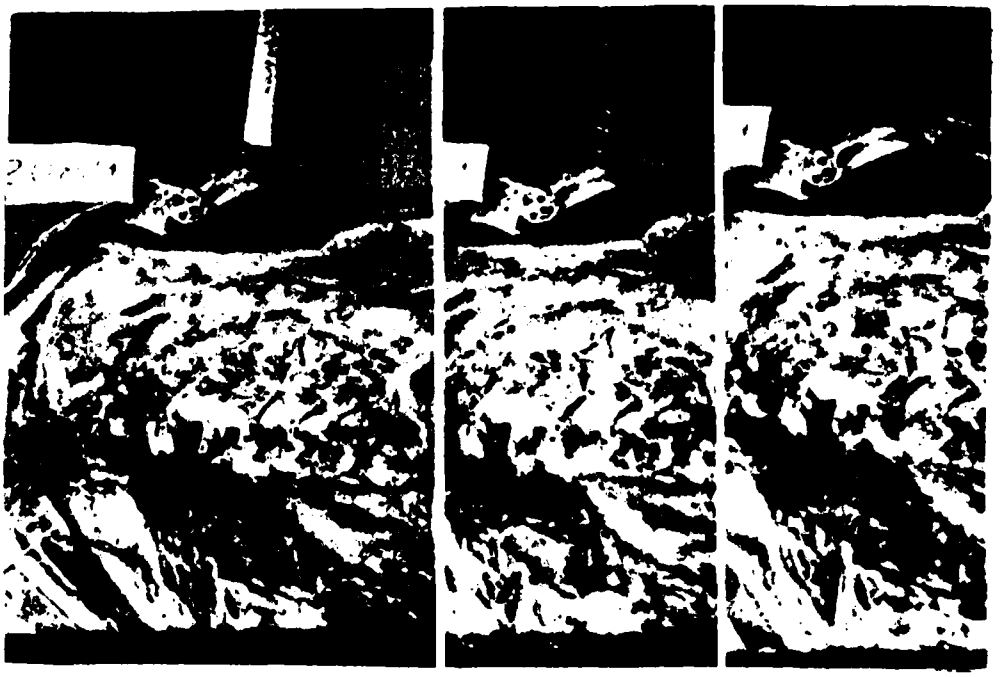

Fig. 7 - Excerpts from film taken at 500 fps showing the rupture and opening of articulating facets C3-C4 due to lateral bending caused by distributed crown loading.

striking surface is smooth and not centered on the smooth, hard helmet, either of which are free to move transverse to the initial line of motion, the result will be a harmless impact in which the head or striking body is deflected sideways, dissipating only a fracture of the kinetic energy of the moving body (also see reference 3).

For these reasons the static setup such as shown in Figure 3 was devised. Axial and anterior loading with the clevis pin locked and free were produced while measuring strain in the anterior surfaces of the body of C3, C5, C7 by means of foil strain gages. Also the cervical spine, were obtained simultaniously as shown in Figure 8. For axial loading of the spine with the clevis fixed, the load is distributed predominantly as axial compression in the cervical spine bodies and facet joints as evident by the relatively straight lower plot. For anterior loading with free clevis, the curve labelled 2 was obtained and evidently results from stretching of the posterior longitudinal ligament and interspinous ligaments as the neck is flexed.

STRAIN DISTRIBUTED FROM STATIC LOADING - In Figure 9a is shown the shape of the cervical spine, diagramatically, under the condition of clevis free, axial loading and initial upper cervical spine extension. The strain distribution under these conditions corresponds to the prediction by Bauze and Ardran (2) from observations of their model, which suggested that if a person landed on his head with the neck in extension, fractured spinous processes and ruptured anterior longitudinal ligaments or anterior avulsion fractures could be expected. The spine shape and strain distribution also correspond to the cadaver damage experienced by Culver, et al. (4).

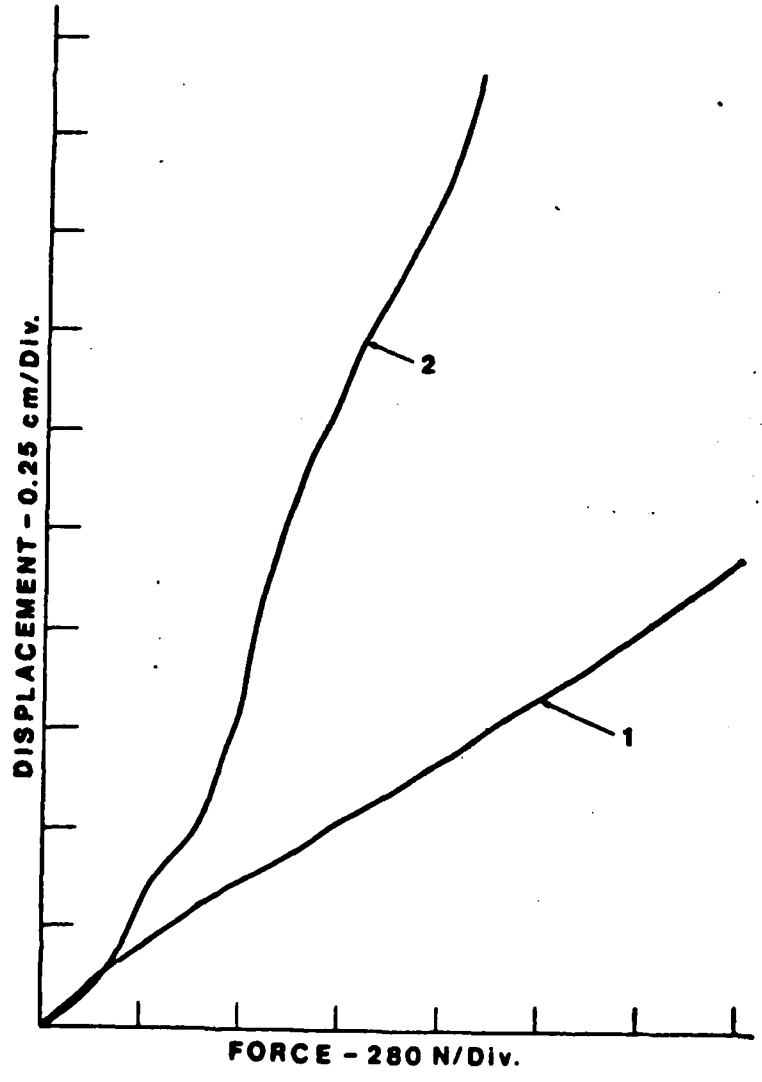

Fig. 8 - Static load deflection due to axial loading with no head rotation ((1) bone loading) and anterior to cervical axis loading with head free to rotate ((2) ligament loading).

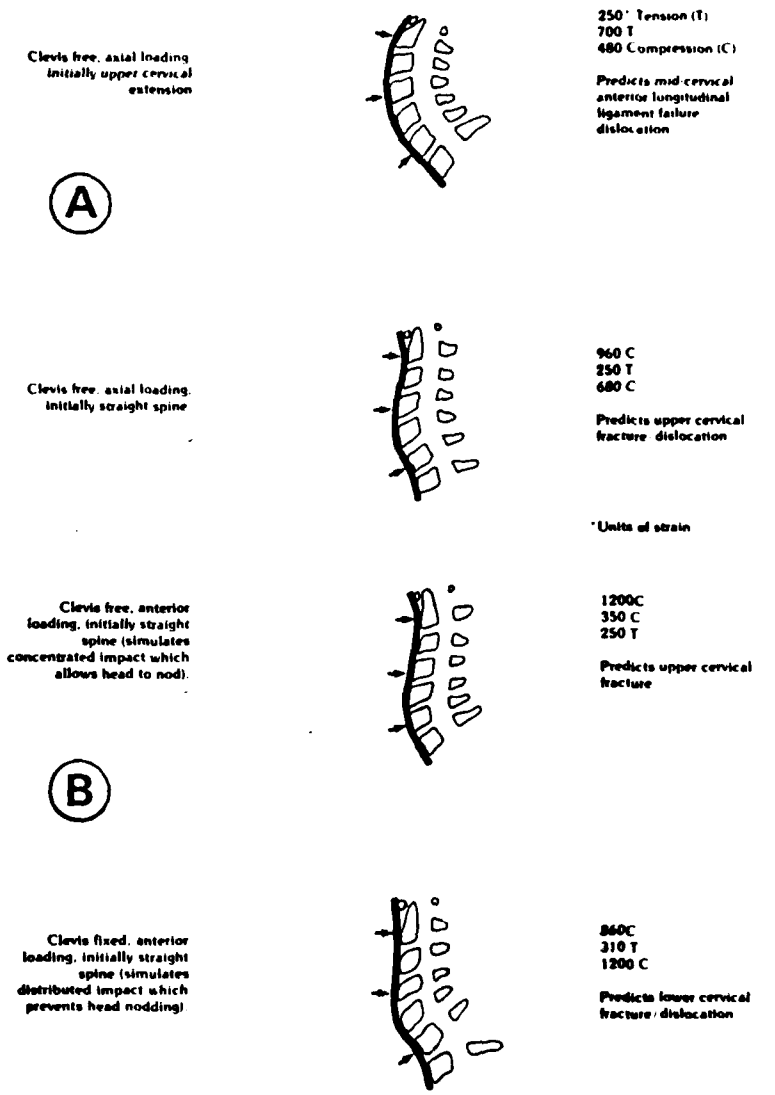

Fig. 9 A & B - Diagrams of curvature and peak strain values for similar maximum load levels (~1.8 kN) under four different loading conditions.

With similar loading of the initially straight spine, flexion occured in the upper cervical spine which produced high compressive strain in C2. The model predicts the likelihood of a forward dislocation of C2 on C3 (Fig. 9b).

As the load is moved anteriorly with the clevis free, flexion in the upper cervical becomes more pronounced with the increased likelihood of either fracture or dislocation in the upper cervical spine at lower load levels (Fig. 9c).

With the clevis fixed, anterior loading, and with initially straight spine, the loading simulates an impact by a distributed surface anterior to the cervical spine which prevents rotation of atlanto-occipital joint (nodding). Moderate compressive loading is experienced in the upper cervical and high compression in C6 just below the inflection point at which the stress in anterior body surfaces changes from tension to compression. The model predicts lower cervical spine fracture and/or dislocation (Fig. 9d).

EFFECT OF HEAD-CERVICAL SPINE-BODY ALIGNMENT WITH LOAD LINE OF ACTION - In Figure 10 are shown three of the spine alignment configurations which were tested. In this series all impacts were centered on the crown and were produced by propelling the load cell into the stationary cadaver as shown in Figure 11. The tests began with the straight alignment of the lowest figure and progressively the cadaver chest and head were raised to the maximum height at which a crown impact could be produced, i.e., higher elevation would produce interference between the chin and the chest, preventing further flexion. The maximum anterior body strains of C3, C5, and C7 are shown on the figure, indicating a progressive severity as the upper arching and, therefore, initial cervical spine

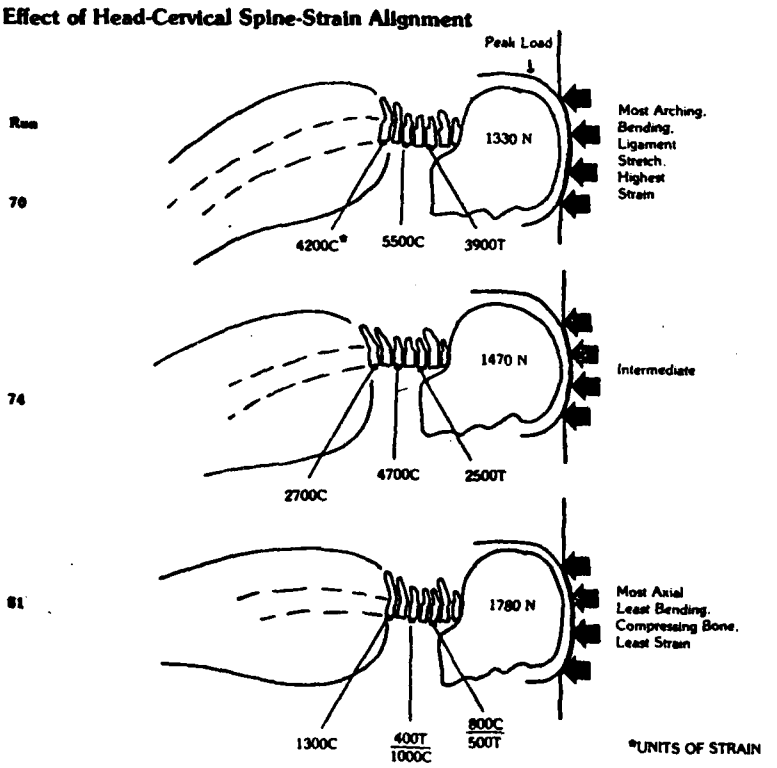

Fig. 10 - Effect of Head-Cervical Spine-Body alignment on anterior cervical body strain.

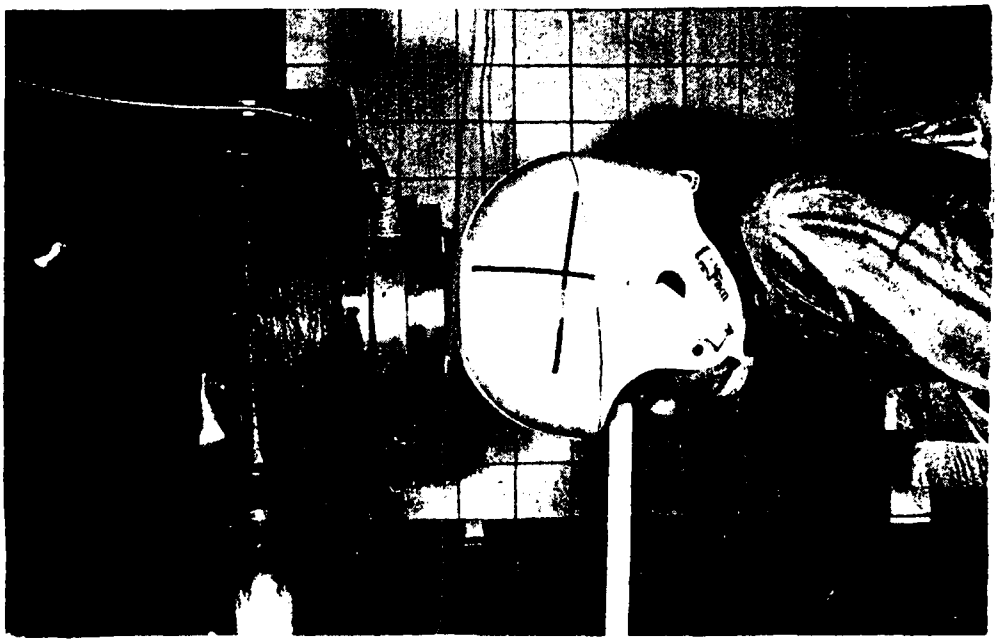

Fig. 11 - Load cells used to deliver padded or unpadded impacts to the cadaver crown.

flexion becomes more pronounced. Because of the straight alignment, the lowest position involved a greater percentage in inertial resistance from body mass below C7, and the highest arched position the least amount, as indicated by the lower force recorded in the latter case. These comparative values of strain point out the difficulty in attempting to ascribe a tolerable force level for crown impact in three positions which would be described as axial loading. The top position which produced significantly higher strain at each of the three strain gage measuring locations, recorded the lowest force on the head.

EFFECT OF LOAD LINE OF ACTION RELATIVE TO THE CERVICAL AXIS - Shown in Figure 12 are the strains recorded for impacts at three locations on the head for a constant chest elevation. The least strain was recorded on the anterior bodies of the vertebrae with the load cell centered 76 mm above the front rim. Maximum levels of strain were recorded for the crown impact centered 191 mm above the front rim of the helmet. Contrasting with the data obtained in Figure 10, minimum strain on the anterior surfaces were recorded here for the minimum load on the head which was obtained for the blow centered near the front of the head. Maximum force and strain were recorded for the crown impact in which there was initially straightest alignment involving a greater amount of body mass below C7, whereas for the nearly frontal blow, the inertial reaction was provided primarily by the mass of the head and the neck. The intermediate position produced intermediate force and strain levels. It can be seen however, that there is not a proportionate increase of strain with load, but rather a precipitous increase in strain with small increase in load, again indicating the difficulties in establishing tolerable load levels for the neck due to head impacts.

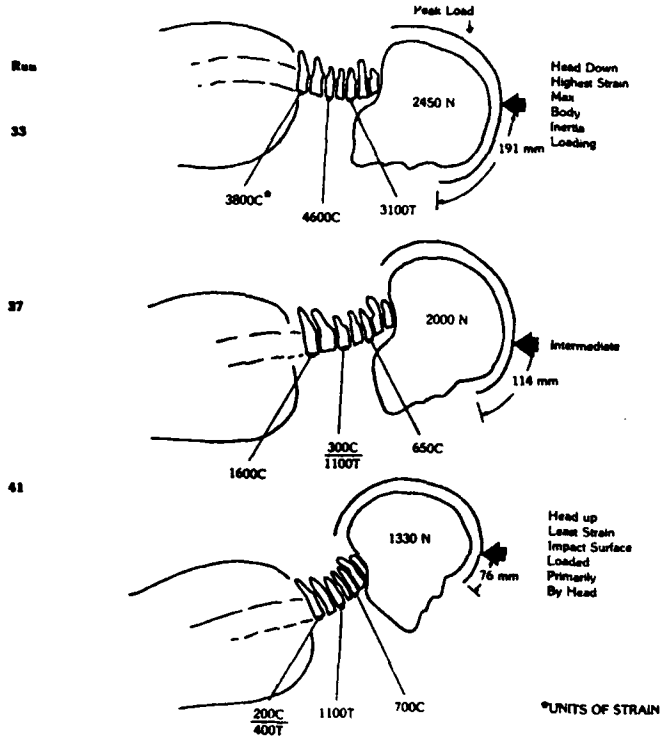

Fig. 12 - Effect of load line of action relative to the cervical spine axis on cervical anterior body strain.

EFFECT OF ENERGY ABSORBING MATERIAL IN THE CROWN - An attempt was made to determine if the strain in the cervical spine could be reduced by means of varying the energy absorbing material on the load cell which struck the crown of the cadaver oriented to produce cervical spine axis alignment as close as possible. Impacts were delivered against the unhelmeted head with no pad on the load cell, producing the load and strains at C3, C5, and C7 as shown for Run 61 in Table 1. A firm, resilient energy absorber, 76 mm thick, was applied to the load cell, with no helmet on the cadaver, producing the loads and strains for Run 68, resulting in slightly higher compressive strains at C5 and C7. When the helmet was placed on the cadaver, and using the same firm padding, strain levels were similar to the no pad, no helmet condition of Run 61, except being slightly lower compressive strains at C7. Essentially the same strains were produced with a soft foam pad of the same thickness and wearing a helmet as shown for Run 72. Apparently the only effect of inserting the padding was to slightly change the shape of the impulse by reducing the peak force and spreading out the time duration. It is assumed that practical amounts of padding did not significantly reduce strain because:

1. The loading is distributed over an area on the order of 26 cm^2, on the helmet surface, consequently, the padding is relatively stiff compared to the spine with which it is in series and does little to modify the loading of the spine.

2. Even when the helmet and energy absorbing material combination acts to alter the peak force, strain is not linearly related in the curved column which is trapped between the head and the body below C7. The critical load at which the cervical spine buckles further out of its initial alignment varies unpredictably due to the factors demonstrated previously in Figures 10 and 12.

Table 1

Crown 'Energy Absorption Inadequate' Theory:

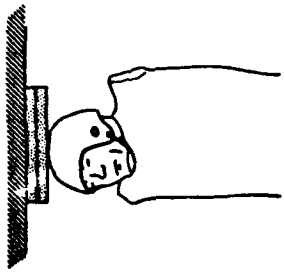

EFFECT OF ENERGY ABSORBER (EA) MATERIAL ON CERVICAL SPINE STRAIN DUE TO CROWN IMPACTS BY 49 Kg MASS

RUN	PAD TYPE	PAD THICKNESS mm	HELMET	PEAK FORCE kN	TENSION C_1	COMPRESSION C_1	C_2
61	no	–	no	2.0	3700	5200	4400
68	Firm,	76	no	1.8	3700	5500	4700
69	Firm	76	yes	1.3	3700	5200	4000
72	Soft	76	yes	1.3	3800	5200	3840
'SILLY PUTTY' COLLAR							
102	NO	–	yes	2.0	700	1600	960

RESULTS:

Practical amounts of padding did not significantly reduce strain because:

1. Axial loading of a straight spine is usually distributed over a large head area ($\simeq 129$ cm^2). Therefore padding is relatively stiff, doesn't dissipate much energy by deformation, and
2. In case of off-axis impact with a curved spine the padding is in series with a softer ligament stretching system over which it has little control.
3. Energy available is much greater than can be absorbed by practical amounts of padding worn on the helmet crown.
4. A 'silly putty' collar was very effective in reducing cervical spine strain. It is assumed to act by stiffening under impact to transfer loads from helmet to shoulder pads and provide a simulated tensed muscle lateral stability.

3. Furthermore, the energy available in these tests or in a propelled body involved in a motor vehicle crash, is usually much greater than can be absorbed with practical amounts of deforming material or structures either worn on the head or mounted in a vehicle, to alleviate strain in the cervical spine due to a crown impact.

As shown for Run 102 in Table 1 the only protective procedure which produced significantly lower strain was by means of a silicon collar ('silly-putty') wrapped around the neck in a plastic bag. The collar had the effect of stiffening on impact to simulate the lateral stability supplied by tensed muscles, and also to transfer the load around the neck from the helmet into the shoulders.

EFFECT OF HELMET REAR RIM IN HYPEREXTENSION INJURIES - There have been many medicolegal ramifications related to the design of the helmet rear rim (crash and football helmets) since Schneider (5) attributed three football neck injuries to a guillotine mechanism of the helmet. According to this theory, an impact to the facemask with an IS compoment of force causes rotation of the helmet on the head, hyperextension of the neck and impingement of the helmet rear rim on the back of the neck with such force as to produce fracture and/or dislocation. Schneider recommended that the rear rim of helmets be cut higher to eliminate this hazard. To test the theory and the remedy, a cadaver was instrumented with seven strain gages on the anterior bodies and near the articulating facets from C2 through C7. The cadaver was strapped to a pallet free to pivot at the feet, and with head overhanging the raised end of the pallet. A Sierra 1050 leg, flexed at the knee, was mounted in the path of the fall of the head such that the facemask would strike the knee about 150 mm above the joint causing hyperextension of the neck of the cadaver as shown in Figure 2. The knee was free to move upon impact.

Preliminary tests on four cadavers with a standard helmet showed that the helmet contacted the rear of the body between C7 and T2 as shown in Figure 13, which is an excerpt taken at 500 fps at the instant of contact of the helmet with the body showing the flag, which is mounted in the spinous process of T2, being bent. Two drops each were conducted with a standard helmet and with a helmet cut high according to the reccomendation. Maximum drop height of the head above the knee was 610 mm. The results of these tests for the maximum drop are shown in Table 2.

The high cut helmet had a padded rim to distribute the load. The standard helmet had a partial suspension (nape bond) inside the rear rim to help maintain clearance between the rim and the neck in the event of hyper-extension motions. High-speed motion pictures showed that both helmets contacted the lower neck. The cross on the helmets rotated through 41 degrees, from initial contact of the knee with the facemask until contact of the helmet rear rim with the neck for the high cut hemlet, and 28 degrees for the standard helmet. At all but one (about equal) strain locations the strain was higher for the high cut helmet. These results would indicate that is is hyperextension of the neck, partially alleviated by the lower cut standard helmet shell interference, which is the determining factor in spinal strain distribution and not contact of the helmet with the neck. Furthermore, the remedy for this alleged mechanism appears to make it more likely that an injury from contact of the rear rim of the helmet with the neck will occur because not only does a higher rim allow more extension but tends to hit higher on the neck and at a greater angle.

CLOSING REMARKS

Although these tests have not been exhaustive of many modes of neck loading which can cause injury, the results indicate that the possibility

Fig. 13 - Rear rim bending flag stuck into T2 due to hyperextension from blow under facemask.

Table 2

'GUILLOTINE' THEORY:

EFFECT OF KNEE TO FACEGUARD IMPACT
STANDARD VS HIGH CUT REAR SHELL RIM-610 mm DROP

	Strain[1] in/in							of Ext. Rotation-deg.
	Facets			Anterior Body				
HELMET	C2	C3	C5	C2	C3	C4	C5	
STANDARD SUSPENSION	-1030	550	-300	-480 150	1100	1140	270	28
HIGH CUT[2] (padded)	-1320	900	-320	-260 260	1380	1330	500	41
% CHANGE	28	64	7	—	24	16	85	46

[1] (-) indicates compression
[2] Done first

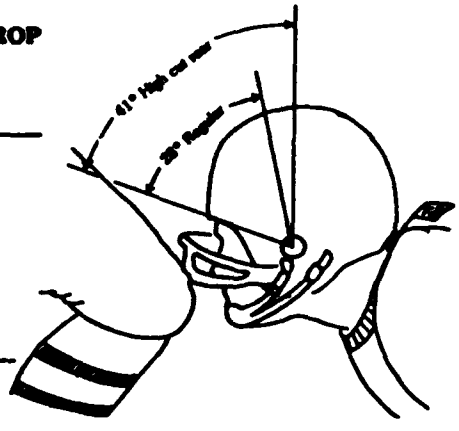

RESULTS:
No injury was produced
Rear rim impinged in C7-T2 area
Higher cutout caused more extension and larger strains

of developing criteria such as tolerable neck loads for the general case of head impact seems unlikely. They suggest that the optimum method of head-face-neck protection for high risk of crash vehicles, and which may become more attractive to the general public with the transition to smaller vehicles, should include a helmet-facemask-neck collar-shoulder pad combination worn by passengers. The neck collar would serve the purpose of transferring loads around the neck in event of crown loading and would also help to limit cervical flexures in all directions.

CONCLUSIONS

1. Distributed crown impacts grip the head, tending to prevent the nodding motion at the atlanto-occipital joint, thereby forcing exaggeration of lower cervical flexion and thereby higher anterior body compression and ligament shear strain, with the likelihood of a fracture and/or dislocation most probable between C4-C7.

2. Concentrated crown impacts allow nodding at the atlanto-occipital junction with the result that dislocation failure in the upper cervical from compression-flexion-shear loading will be the threshold injury.

3. For crown impacts with a flat rigid impactor, the greatest risk of injury occurs when the body-cervical spine axis-head alignment is in a flexure posture prior to impact. The minimum risk occurs when the body-cervical spine and head are in alignment (near axial loading).

4. For impacts to the head with a flat rigid impactor, maximum risk of injury to the neck, holding the orientation of the spine below C7 constant, occurs for a crown impact; minimum risk for a forehead impact.

5. Firm or soft energy absorbing materials up to 76 mm did not reduce strain due to a crown impact with a flat rigid impactor.

6. The posterior rim guillotine injury mechanism theory was not validated by these experiments and the remedy of cutting the helmet higher appears to make the possiblilty of injury from this mechanism more likely to occur.

7. Crown loading was not found to correlate with cervical spine strain.

ACKNOWLEDGMENTS

This work was sponsored in part by the National Operating Committee on Standards for Athletic Equipment (NOCSAE), Detroit General Hospital Research Corporation, and the Office of Naval Research.

Eugene Dupuis conducted the surgery and instrumentation of the cadavers. Matthew Mason was responsible for the photography and Robert Neumann assisted in the experiments.

REFERENCES

1. R. Roaf, "A Study of the Mechanics of Spinal Injury." The Journal of Bone and Joint Surgery, Volume 42B, Number 2, November 1960.

2. J. R. Bauze, and M. A. Ardran, "Experimental Production of Forward Dislocation in the Human Cervical Spine." The Journal of Bone and Joint Surgery, Volume 60B, Number 2, May 1978.

3. H. J. Mertz, V. R. Hodgson, L. M. Thomas, and G. W. Nyquist, "An Assessment of Compressive Neck Loads Under Injury-Producing Conditions." The Physicial and Sportsmedicine, Volume 6, Number 11, November 1978.

4. R. H. Culver, M. Bender, and J. W. Melvin, "Mechanisms, Tolerance, and Responses Obtained Under Dynamic Superior-Inferior Head Impact." OSHA Final Report, May 1987.

5. R. C. Schneider, "Head and Neck Injuries in Football, Mechanisms, Treatment, and Prevention." Baltimore, MD: Williams and Wilkins, 1973.

...ALIFIED AND OTHER TECHNICAL COLLABORATORS

Universities

Dr. J. Tinsley Oden
University of Texas at Austin
ASE Eng. Science Bldg
Austin, Texas 78712

Prof. Julius Miklowitz
California Institute of Technology
Div. of Engineering & Applied Sciences
Pasadena, California 91109

Dr. Harold Liebowitz, Dean
School of Engr. & Applied Science
George Washington University
725 23rd St. N.W.
Washington, D.C. 20006

Prof. Ell Sternberg
California Institute of Technology
Div. of Engr. & Applied Sciences
Pasadena, California 91109

Prof. Paul M. Naghdi
University of California
Div. of Applied Mechanics
Etcheverry Hall
Berkeley, California 94720

Professor P.S. Symonds
Brown University
Division of Engineering
Providence, R.I. 02912

Prof. A.J. Durelli
The Catholic University of America
Civil/Mechanical Engineering
Washington, D.C. 20017

Prof. B.B. Tosta
Columbia University
Dept. of Civil Engineering
S.W. Mudd Bldg.
New York, N.Y. 10027

Prof. H.H. Bleich
Columbia University
Dept. of Civil Engineering
Amsterdam & 120th St.
New York, N.Y. 10027

Prof. P.L. DiMaggio
Columbia University
Dept. of Civil Engineering
616 Mudd Building
New York, N.Y. 10027

Prof. A.M. Freudenthal
George Washington University
School of Engineering & Applied Science
Washington, D.C. 20006

D.C. Evans
University of Utah
Computer Science Division
Salt Lake City, Utah 84112

Prof. Norman Jones
Massachusetts Inst. of Technology
Dept. of Naval Architecture & Marine Engineering
Cambridge, Massachusetts 02139

Professor Albert I. King
Biomechanics Research Center
Wayne State University
Detroit, Michigan 48202

Dr. V.H. Hodgson
Wayne State University
School of Medicine
Detroit, Michigan 48202

Dean B.A. Boley
Northwestern University
Technological Institute
2145 Sheridan Road
Evanston, Illinois 60201

Prof. P.G. Hodge, Jr.
University of Minnesota
Dept. of Aerospace Engr. & Mechanics
Minneapolis, Minnesota 55455

Dr. D.C. Drucker
University of Illinois
Dean of Engineering
Urbana, Illinois 61801

Prof. N.M. Newmark
University of Illinois
Dept. of Civil Engineering
Urbana, Illinois 61801

Prof. E. Reissner
University of California, San Diego
Dept. of Applied Mechanics
La Jolla, California 92037

Prof. William A. Nash
University of Massachusetts
Dept. of Mechanics & Aerospace Engr.
Amherst, Massachusetts 01002

Library (Code 0384)
U.S. Naval Postgraduate School
Monterey, California 93940

Prof. Arnold Allentuch
Newark College of Engineering
Dept. of Mechanical Engineering
323 High Street
Newark, New Jersey 07102

Dr. George Herrmann
Stanford University
Dept. of Applied Mechanics
Stanford, California 94305

Prof. J.D. Achenbach
Northwestern University
Dept. of Civil Engineering
Evanston, Illinois 60201

Director, Applied Research Lab
Pennsylvania State University
P.O. Box 30
State College, Pennsylvania 16801

Prof. Eugen J. Skudrzyk
Pennsylvania State University
Applied Research Laboratory
Dept. of Physics - P.O. Box 30
State College, Pennsylvania 16801

Prof. J. Kempner
Polytechnic Institute of Brooklyn
Dept. of Aero. Engr. & Applied Mech.
333 Jay Street
Brooklyn, N.Y. 11201

Prof. J. Klosner
Polytechnic Institute of Brooklyn
Dept. of Aerospace & Appl. Mech.
333 Jay Street
Brooklyn, N.Y. 11201

Prof. E.A. Schapery
Texas A&M University
Dept. of Civil Engineering
College Station, Texas 77840

Prof. W.D. Pilkey
University of Virginia
Dept. of Aerospace Engineering
Charlottesville, Virginia 22903

Dr. H.C. Schaeffer
University of Maryland
Aerospace Engineering Dept.
College Park, Maryland 20742

Prof. R.D. Williams
Clarkson College of Technology
Dept. of Mechanical Engineering
Potsdam, N.Y. 13676

Dr. J.A. Strickle
Texas A&M University
Aerospace Engineering Dept.
College Station, Texas 77843

Dr. L.A. Schmit
University of California, LA
School of Engineering & Applied Science
Los Angeles, California 90024

Dr. E.A. Kamel
The University of Arizona
Aerospace & Mech. Engineering Dept.
Tucson, Arizona 85721

Dr. E.S. Berger
University of Maryland
Dept. of Mechanical Engineering
College Park, Maryland 20742

Prof. G.R. Irwin
Dept. of Mechanical Engineering
University of Maryland
College Park, Maryland 20742

Dr. S.J. Fenves
Carnegie-Mellon University
Dept. of Civil Engineering
Schenley Park
Pittsburgh, Pennsylvania 15213

Dr. Ronald L. Huston
Dept. of Engineering Analysis
Mail Box 112
University of Cincinnati
Cincinnati, Ohio 45221

Prof. George Sih
Dept. of Mechanics
Lehigh University
Bethlehem, Pennsylvania 18015

Prof. A.S. Kobayashi
University of Washington
Dept. of Mechanical Engineering
Seattle, Washington 98195

Librarian
Webb Institute of Naval Architecture
Crescent Beach Road, Glen Cove
Long Island, New York 11542

Prof. Daniel Frederick
Virginia Polytechnic Institute
Dept. of Engineering Mechanics
Blacksburg, Virginia 24061

Prof. A.C. Eringen
Dept. of Aerospace & Mech. Sciences
Princeton University
Princeton, New Jersey 08540

Dr. S.L. Koh
School of Aero., Astro. & Engr. Sci
Purdue University
Lafayette, Indiana

Prof. E.H. Lee
Div. of Engr. Mechanics
Stanford University
Stanford, California 94305

Prof. H.D. Hibbitt
Dept. of Civil Engineering
Columbia University
S.W. Mudd Building
New York, N.Y. 10027

Prof. S.B. Dong
University of California
Dept. of Mechanics
Los Angeles, California 90024

Prof. Burt Paul
University of Pennsylvania
Towne School of Civil & Mech. Engr.
Rm. 113 - Towne Building
220 S. 33rd Street
Philadelphia, Pennsylvania 19104

Prof. W.W. Liu
Dept. of Chemical Engineering & Metall.
Syracuse University
Syracuse, N.Y. 13210

Prof. S. Ben-Israel
Technion Res. Foundation
Haifa, Israel

Prof. R.J.H. Bollard
Chairman, Aeronautical Engr. Dept.
207 Guggenheim Hall
University of Washington
Seattle, Washington 98195

Prof. G.S. Ballof
Division of Engineering
Brown University
Providence, Rhode Island 02912

Prof. Werner Goldsmith
Dept. of Mechanical Engineering
Div. of Applied Mechanics
University of California
Berkeley, California 94720

Prof. J.R. Rice
Division of Engineering
Brown University
Providence, Rhode Island 02912

Prof. R.S. Rivlin
Center for the Application of Mathematics
Lehigh University
Bethlehem, Pennsylvania 18015

Library (Code 0384)
U.S. Naval Postgraduate School
Monterey, California 93940

Dr. Francis Cozzarelli
Div. of Interdisciplinary Studies & Research
School of Engineering
State University of New York
Buffalo, N.Y. 14214

Industry and Research Institutes

Library Services Department
Report Section Bldg. 14-14
Argonne National Laboratory
9700 S. Cass Avenue
Argonne, Illinois 60440

Dr. M.C. Junger
Cambridge Acoustical Associates
129 Mount Auburn St.
Cambrige, Massachusetts 02138

Dr. L.H. Chen
General Dynamics Corporation
Electric Boat Division
Groton, [illegible]

Dr. J.P. [illegible]
J.G. Engineering Research Associates
3831 Menlo Drive
Baltimore, Maryland 21215

Dr. S. Batdorf
The Aerospace Corp
P.O. Box 92957
Los Angeles, California 90009

Dr. E.C. Park
Lockheed Palo Alto Research Laboratory
Dept. 5233, Bldg. 205
3251 Hanover Street
Palo Alto, California 94304

Library
Newport News Shipbuilding and Dry Dock Co.
Newport News, Virginia 23607

Dr. W.F. Bozich
McDonnell Douglas Corporation
5301 Bolsa Ave
Huntington Beach, California 92647

Dr. H.H. Abramson
Southwest Research Institute
Technical Vice President
Mechanical Sciences
P.O. Drawer 28510
San Antonio, Texas 78284

Dr. R.C. DeHart
Southwest Research Institute
Dept. of Structural Research
PO Drawer 28510
San Antonio, Texas 78284

Dr. M.L. Baron
Weidlinger Associates,
Consulting Engineers
110 East 59th Street
New York, N.Y. 10022

Dr. W.A. von Riesemann
Sandia Laboratories
Sandia Base
Albuquerque, New Mexico 87115

Dr. T.L. Geers
Lockheed Missiles & Space Co.
Palo Alto Research Laboratory
3251 Hanover Street
Palo Alto, California 94304

Dr. J.E. Tucker
Boeing Computer Services, Inc.
P.O. Box 24346
Seattle, Washington 98124

Dr. William Caywood
Code 5502, Applied Physics Laboratory
8621 Georgia Avenue
Silver Spring, Maryland 20910

Mr. P.C. Durup
Lockheed-California Company
Aeromechanics Dept. (74-43)
Burbank, California 91503

Addendum

Assistant Chief for Technology
Office of Naval Research, Code 200
Arlington, Virginia 22217

PART 1 - GOVERNMENT

<u>Administrative & Liaison Activities</u>

Chief of Naval Research
Department of the Navy
Arlington, Virginia 22217
  Attn: Code 474 (2)
         471
         222

Director
ONR Branch Office
495 Summer Street
Boston, Massachusetts 02210

Director
Naval Research Laboratory
[illegible] 579 (ONRL)
[illegible] 20390 (6)

U.S. Naval Research Laboratory
Attn: Code 2627
Washington, D.C. 20390

Director
ONR - New York Area Office
715 Broadway - 5th Floor
New York, N.Y. 10003

Director
ONR Branch Office
1030 E. Green Street
Pasadena, California 91101

Defense Documentation Center
Cameron Station
Alexandria, Virginia 22314 (12)

Army

Commanding Officer
U.S. Army Research Office Durham
Attn: Mr. J.J. Murray
CRD-AA-IP
Box CM, Duke Station
Durham, North Carolina 27706 (2)

Commanding Officer
AMXMR-ATL
Attn: Mr. R. Shea
US Army Materials Res. Agency
Watertown, Massachusetts 02172

Watervliet Arsenal
MAGGS Research Center
Watervliet, New York 12189
  Attn: Director of Research

Techical Library

Redstone Scientific Info. Center
Chief, Document Section
U.S. Army Missile Command
Redstone, Arsenal, Alabama 35809

Army R&D Center
Fort Belvoir, Virginia 22060

<u>Navy</u>

Commanding Officer and Director
Naval Ship Research & Development Center
Bethesda, Maryland 20034
  Attn: Code 042 (Tech. Lib. Br.)
         17
         172
         174
         177
         1800 (Appl. Math. Lab.)
         5412S (Dr. W.D. Sette)
         19
         1901 (Dr. M. Strassberg)
         1945
         196
         1962

Naval Weapons Laboratory
Dahlgren, Virginia 22448

Naval Research Laboratory
Washington, D.C. 20375
  Attn: Code 8400
         8410
         8430
         8440
         6300
         6390
         6380

Undersea Explosion Research Div.
Naval Ship R&D Center
Norfolk Naval Shipyard
Portsmouth, Virginia 23709
  Attn: Dr. E. Palmer
        Code 780

Naval Ship Research & Development Center
Annapolis Division
Annapolis, Maryland 21402
  Attn: Code 2740 - Dr. Y.F. Wang
              28 - Mr. R.J. Wolfe
             281 - Mr. R.B. Niederberger
            2814 - Dr. H. Vanderveldt

Technical Library
Naval Underwater Weapons Center
Pasadena Annex
3202 E. Foothill Blvd.
Pasadena, California 91107

U.S. Naval Weapons Center
China Lake, California 93557
  Attn: Code 4062 - Mr. W. Werback
              4520 - Mr. Ken Bischel

Commanding Officer
U.S. Naval Civil Engr. Lab
Code L31
Port Hueneme, California 93041

Technical Director
U.S. Naval Ordnance Laboratory
White Oak
Silver Spring, Maryland 20910

Technical Director
Naval Undersea R&D Center
San Diego, California 92132

Supervisor of Shipbuilding
U.S. Navy
Newport News, Virginia 23607

Technical Director
Mare Island Naval Shipyard
Vallejo, California 94592

U.S. Navy Underwater Sound Ref. Lab.
Office of Naval Research
PO Box 8337
Orlando, Florida 32806

Chief of Naval Operations
Dept. of the Navy
Washington, D.C. 20350
  Attn: Code Op07T

Strategic Systems Project Office
Department of the Navy
Washington, D.C. 20390
  Attn: NSP-001 Chief Scientist

Deep Submergence Systems
Naval Ship Systems Command
Code 39522
Department of the Navy
Washington, D.C. 20360

Engineering Dept.
US Naval Academy
Annapolis, Maryland 21402

Naval Air Systems Command
Dept. of the Navy
Washington, D.C. 20360
  Attn: NAVAIR 5302 Aero & Structures
              5308 Structures
              52031F Materials
              604 Tech. Library
              320B Structures

Director, Aero Mechanics
Naval Air Development Center
Johnsville
Warminster, Pennsylvania 18974

Technical Director
U.S. Naval Undersea R&D Center
San Diego, California 92132

Engineering Department
U.S. Naval Academy
Annapolis, Maryland 21402

Naval Facilities Engineering Command
Dept. of the Navy
Washington, D.C. 20360
  Attn: NAVFAC 03 Research & Development
              04 " "
              14114 Tech. Library

Naval Sea Systems Command
Dept. of the Navy
Washington, D.C. 20360
  Attn: NAVSHIP 03 Res. & Technology
              031 Ch. Scientist for R&D
              03412 Hydromechanics
              037 Ship Silencing Div.
              035 Weapons Dynamics

Naval Ship Engineering Center
Prince Georges' Plaza
Hyattsville, Maryland 20782
  Attn: NAVSEC 6100 Ship Sys. Engr. & Des. Dep.
              6102C Computer-Aided Ship Des.
              6105G
              6110 Ship Concept Design
              6120 Hull Div.
              6120D Hull Div.
              6128 Surface Ship Struct.
              6129 Submarine Struct.

<u>Air Force</u>

Commander WADD
Wright-Patterson Air Force Base
Dayton, Ohio 45433
  Attn: Code WWRMDD
         AFFDL (FDDS)
         Structures Division
         AFLC (MCEEA)

Chief, Applied Mechanics Group
U.S. Air Force Inst. of Tech.
Wright-Patterson Air Force Base
Dayton, Ohio 45433

Chief, [illegible] Engineering Branch
[illegible] Research Division
[illegible] Weapons Laboratory
Kirtland AFB, New Mexico 87117

[illegible] Office of Scientific Research
[illegible]
[illegible], Virginia 22209
Attn: Mechanics Div.

[illegible]

[illegible] Research Division
[illegible] Aeronautics & Space Admin.
[illegible] Research Center
[illegible]
[illegible], Virginia 23365

[illegible] Aeronautics & Space Admin.
[illegible] Administrator for Advanced
[illegible] & Technology
[illegible] D.C. 20546

[illegible] & Tech. Info. Facility
[illegible] Representative (S-AK/DL)
[illegible]
[illegible] Maryland 20014

<u>Other Government Activities</u>

[illegible]
[illegible] Development Div.
[illegible]
[illegible]
[illegible]

[illegible] Director
[illegible] Dev. & Eng. Command
[illegible], Virginia 22134

Director
National Bureau of Standards
Washington, D.C. 20234
  Attn: Mr. B.L. Wilson, EM 219

Dr. M. Gaus
National Science Foundation
Engineering Division
Washington, D.C. 20550

Science & Tech. Division
Library of Congress
Washington, D.C. 20540

Director
Defense Nuclear Agency
Washington, D.C. 20305
  Attn: SPSS

Commander Field Command
Defense Nuclear Agency
Sandia Base
Albuquerque, New Mexico 87115

Director Defense Research & Engrg.
Technical Library
Room 3C-128
The Pentagon
Washington, D.C. 20301

Chief, Airframe & Equipment Branch
FS-120
Office of Flight Standards
Federal Aviation Agency
Washington, D.C. 20553

Chief, Research and Development
Maritime Administration
Washington, D.C. 20235

Deputy Chief, Office of Ship Construction
Maritime Administration
Washington, D.C. 20235
  Attn: Mr. U.L. Russo

Atomic Energy Commission
Div. of Reactor Devel. & Tech.
Germantown, Maryland 20767

Ship Hull Research Committee
National Research Council
National Academy of Sciences
2101 Constitution Avenue
Washington, D.C. 20418
  Attn: Mr. A.R. Lytle


DATE
IL ME